

Structure and Function of Transient Encounters of Redox Proteins

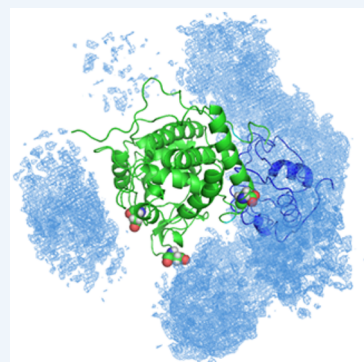
Alexander N. Volkov*

Jean Jeener NMR Centre, Structural Biology Brussels, Vrije Universiteit Brussel, and Structural Biology Research Center, VIB, Pleinlaan 2, 1050 Brussels, Belgium

CONSPECTUS: Many biomolecular interactions proceed via lowly populated, transient intermediates. Believed to facilitate formation of a productive complex, these short-lived species are inaccessible to conventional biophysical and structural techniques and, until recently, could only be studied by theoretical simulations. Recent development of experimental approaches sensitive to the presence of minor species—in particular paramagnetic relaxation enhancement (PRE) NMR spectroscopy—has enabled direct visualization and detailed characterization of such lowly populated states. Collectively referred to as an encounter complex, the binding intermediates are particularly important in transient protein interactions, such as those orchestrating signaling cascades or energy-generating electron transfer (ET) chains.

Here I discuss encounter complexes of redox proteins mediating biological ET reactions, which are essential for many vital cellular activities including oxidative phosphorylation and photosynthesis. In particular, this Account focuses on the complex of cytochrome *c* (Cc) and cytochrome *c* peroxidase (CcP), which is a paradigm of biomolecular ET and an attractive system for studying protein binding and enzymatic catalysis. The Cc-CcP complex formation proceeds via an encounter state, consisting of multiple protein–protein orientations sampled in the search of the dominant, functionally active bound form and exhibiting a broad spatial distribution, in striking agreement with earlier theoretical simulations. At low ionic strength, CcP binds another Cc molecule to form a weak ternary complex, initially inferred from kinetics experiments and postulated to account for the measured ET activity. Despite strenuous efforts, the ternary complex could not be observed directly and remained eagerly sought for the past two decades. Very recently, we have solved its structure in solution and shown that it consists of two binding forms: the dominant, ET-inactive geometry and an ensemble of lowly populated species with short separations between Cc and CcP cofactors, which summarily account for the measured ET rate.

Unlike most protein complexes, which require accurate alignment of the binding surfaces in a single, well-defined orientation to carry out their function, redox proteins can form multiple productive complexes. As fast ET will occur any time the redox centers of the binding partners are close enough to ensure efficient electron tunneling across the interface, many protein–protein orientations are expected to be ET active. The present analysis confirms that the low-occupancy states can support the functional ET activity and contribute to the stability of redox protein complexes. As illustrated here, boundaries between the dominant and the encounter forms become blurred for many dynamic ET systems, which are more aptly described by ensembles of functionally and structurally heterogeneous bound forms.



As recognized for a long time,¹ many biomolecular interactions involve formation of lowly populated, short-lived intermediates. Collectively referred to as an “encounter complex” or “encounter state”,² the binding intermediates are particularly important in transient protein interactions, such as those orchestrating signaling cascades or energy-generating electron transfer (ET) chains. In these systems, fast relay of a message—be it a chemical group, an electron, or a structural change—necessitates short lifetimes of the constituent protein–protein complexes, implying fast dissociation rates (k_{off}) and high dissociation constants (K_D). ($K_D = k_{\text{off}}/k_{\text{on}}$, where k_{off} and k_{on} are the dissociation and association rates, respectively.) Interestingly, in contrast to standard, high-affinity protein complexes,³ transient complexes feature low geometric complementarity and loose packing of the interface, believed to promote fast dissociation.⁴

Recent development of experimental approaches sensitive to the presence of minor species—in particular paramagnetic

relaxation enhancement (PRE) NMR spectroscopy—has enabled direct visualization and detailed characterization of protein encounters.^{5,6} The PRE is caused by a dipolar interaction between a nucleus and unpaired electron(s) of the paramagnetic center, either present in the native protein or introduced into the molecular frame by bioconjugation techniques. Because of the large magnetic moment of the electron and the r^{-6} distance dependence, the transverse ^1H PRE (Γ_2) is a long-range effect, which can extend up to 35 Å and is exquisitely sensitive to the presence of minor species.^{5,6}

Here I discuss transient encounters of redox proteins mediating biological ET reactions, which are essential for many cellular activities including oxidative phosphorylation and photosynthesis—two processes underlying the conversion of energy from food or sunlight into the chemical energy of ATP.

Received: July 27, 2015

Published: November 25, 2015

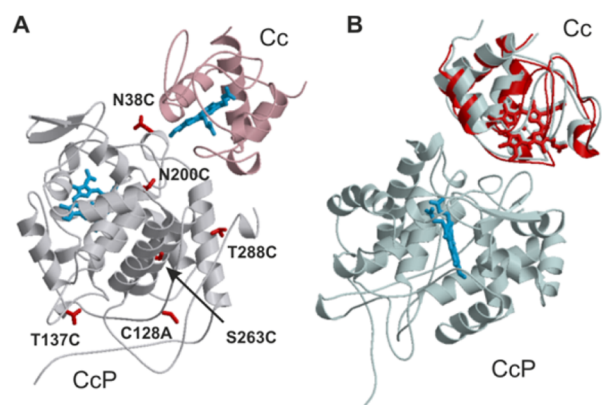


Figure 1. High-affinity Cc-CcP complex. (A) X-ray structure of the complex (PDB entry 2PCC).⁸ Five SL attachment sites and the native C128, replaced by alanine, are colored red and labeled. Heme groups are shown in sticks (B) Comparison of the solution and crystal structures, aligned by CcP. With backbone rmsd of 2.2 Å, the Cc molecules in the best solution and crystal structures are in red and gray, respectively. Reprinted from ref 10. Copyright (2006) National Academy of Sciences, U.S.A.

In particular, this Account focuses on the complex of cytochrome *c* (Cc) and cytochrome *c* peroxidase (CcP), which is a paradigm of biomolecular ET. Located in yeast mitochondria, CcP is a heme enzyme, which reduces hydroperoxides using the electrons provided by its physiological partner Cc. The catalytic mechanism of H₂O₂ reduction involves formation of CcP compound I (CpdI), an intermediate oxidized two equivalents above the CcP(Fe³⁺) resting state and containing the Fe(IV)=O heme oxyferryl and the W191⁺ cation radical.⁷ Subsequent CpdI reduction in two one-electron steps involves complex formation with ferrous Cc, intermolecular ET, and the product dissociation. Extensively studied by different biochemical and biophysical techniques, including X-ray crystallography (Figure 1A),⁸ the Cc-CcP complex is an attractive system for investigating protein–protein interactions, long-range ET, and enzymatic catalysis.^{7,9}

■ A JOURNEY TO THE Cc-CcP ENCOUNTERS

The First Glimpse

Early theoretical and experimental work (reviewed in ref 7) provided evidence for dynamics in the Cc-CcP complex and suggested the presence of alternative, minor binding forms. However, the first direct observation of transient Cc-CcP encounters dates back to the 2006 study,¹⁰ initially intended to establish whether the crystallographic protein–protein orientation was maintained in solution. To obtain distance restraints for the Cc-CcP structure calculation, a nitroxide spin-label (SL) was introduced at five positions on the CcP surface (one at a time, Figure 1A), and intermolecular PREs on the Cc nuclei were measured. Subsequent refinement of the protein complex against the experimental data consistently produced a single, well-defined solution, highly similar to the crystallographic binding geometry (Figure 1B). This finding confirmed that the X-ray structure of the Cc-CcP complex represents the dominant bound form in solution. Indeed, intermolecular PREs back-calculated from the X-ray structure account for most of the observed effects (compare blue and black traces in Figure 2).

However, the experimental PRE profiles also featured additional contributions (highlighted in Figure 2). Clustered in several regions, these extra PREs could not be rationalized by the

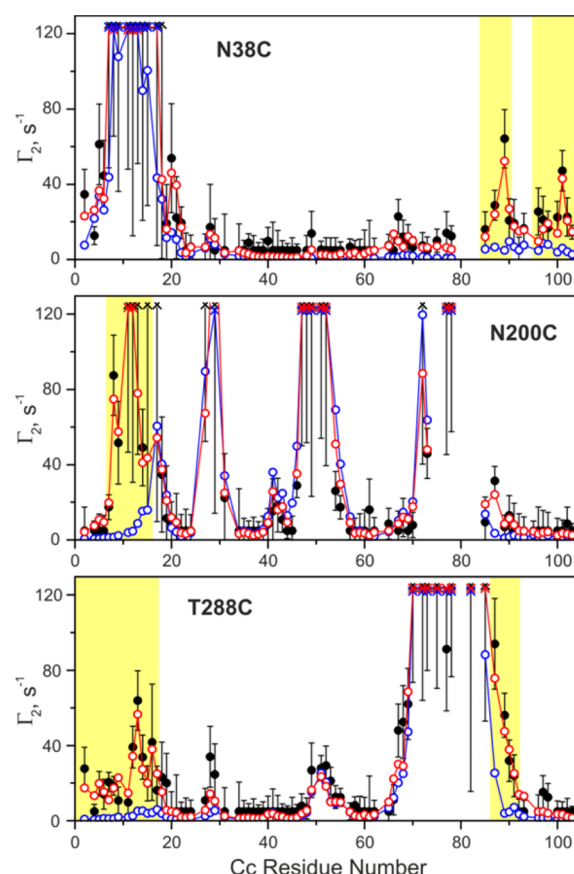


Figure 2. Intermolecular PREs for the Cc-CcP-SL complexes. The plots show experimental $\Gamma_{2,\text{obs}}$ (black), $\Gamma_{2,\text{dom}}$ back-calculated from the X-ray structure of the complex (blue), and $\Gamma_{2,\text{tot}}$ for the combination of the dominant form and an encounter ensemble (red) for three SL attachment sites. Crosses indicate the values of $\Gamma_2 \geq 125 \text{ s}^{-1}$ for the calculated PREs or identify the residues whose resonances disappear in the paramagnetic spectrum. The errors are standard deviations. The regions with additional PREs, not accounted for by the single dominant form, are highlighted in yellow. Reprinted from ref 13. Copyright (2010) by the authors.

crystallographic orientation, where the Cc nuclei in question are too far from the CcP-SL to experience such strong effects. Despite multiple refinement rounds, a single Cc-CcP structure accounting for all observed PREs could not be found. At first, the disagreement between the experimental and the back-predicted Γ_2 values—manifested by several large violations in structure calculations—was seen as an undesirable artifact. This was followed by a realization that the additional effects must arise from alternative, lowly populated protein–protein orientations sampled during the Cc-CcP interaction. Indeed, if the electron–nucleus distance in the minor form is shorter than that in the dominant one, owing to the $\langle r^{-6} \rangle$ distance dependence the former will give rise to a large PRE, making a measurable contribution to the overall, population-weighted Γ_2 value. This interpretation was reinforced by contemporaneous studies of Clore and co-workers,^{11,12} who convincingly showed that such extra PREs are indeed the footprint of transient intermediates in biomolecular binding.

Thus, this early work established that the Cc-CcP complex in solution consists of a dominant protein–protein orientation, the one also seen in the X-ray structure, and minor binding forms, directly detected by PRE NMR spectroscopy. At this point, detailed visualization of transient protein encounters was

not attempted. Instead, a simple geometric analysis was performed to delineate the CcP-centered spatial regions around the SLs yielding additional paramagnetic effects (N38C, N200C, and T288C; Figure 1A) and those showing no PREs at all (S263C and T137C; Figure 1A), which must harbor or exclude the minor species, respectively. Large part of the conformational space remained a “grey zone” not covered by the SL reporters, indicating an insufficient experimental sampling.

Pursuing the Minor Species

In a follow up work,¹⁴ the experimental coverage was increased to a total of 10 SLs, nearly uniformly distributed over the CcP surface, and semiquantitative analysis of protein encounters was performed. First, the interaction between oppositely charged Cc and CcP was simulated ab initio with a Monte Carlo (MC) protocol, combining Poisson–Boltzmann electrostatic calculations and an exclusion grid to avoid steric overlap between the molecules. In this way, an ensemble of protein–protein orientations, mimicking the encounter state, was generated. Second, the intermolecular PREs were back-calculated for each constituent Cc–CcP orientation, averaged over the entire ensemble, and combined with those of the dominant, crystallographic form to obtain the total, population-weighted value: $\Gamma_{2,\text{tot}} = p\Gamma_{2,\text{enc}} + (1 - p)\Gamma_{2,\text{dom}}$, where p is the fractional population of the encounter state. Finally, the best fit between the $\Gamma_{2,\text{tot}}$ and the experimental PRE data ($\Gamma_{2,\text{obs}}$) was found at $p = 0.3$, indicating that 70% of the lifetime of the Cc–CcP complex is spent in the dominant form and 30% in the encounter.¹⁴ Being the result of theoretical simulations, rather than direct refinement against experimental data, the MC solutions nevertheless provide a good approximation of the encounter state and offer a robust estimate of its population (see below).

In the next study,¹³ we performed direct, unbiased, refinement of Cc–CcP encounters using theoretical and computational framework developed by Clore and co-workers.^{5,12,15} To define an ensemble of protein–protein orientations constituting the encounter state, several copies of Cc were docked simultaneously to the CcP molecule, and the agreement between $\Gamma_{2,\text{tot}}$ and $\Gamma_{2,\text{obs}}$ was quantified. To account for the flexibility of the attached paramagnetic probes, the effects were averaged over multiple SL conformations.¹⁵ By varying the number of the docked Cc molecules and the overall encounter population in multiple refinement runs, we found the solution showing best agreement with the experimental PRE data (compare red and black traces in highlighted regions, Figure 2) and confirming the value of $p = 0.3$ obtained in our earlier work.¹⁴

In parallel, we developed a statistically rigorous approach to assess the experimental coverage and delineate the conformational space sampled in the encounter state.¹³ Using this methodology, we validated the distribution of protein–protein orientations obtained with the ensemble refinement protocol and showed that the present $\Gamma_{2,\text{obs}}$ data set was insufficient for complete spatial coverage of the Cc–CcP interaction. It appears that even 10 SLs, nearly uniformly distributed over the CcP surface, are not enough for an adequate experimental sampling of transient protein encounters.¹³ Thus, at this point, we could not exclude that additional Cc–CcP orientations, not reported upon by the current SL set, might complement the solutions of the ensemble refinement.

Mapping out the Encounter State

As illustrated in Figure 3A, the undersampling problem is particularly acute in the current labeling scheme, where paramagnetic probes are attached to the larger protein, CcP,

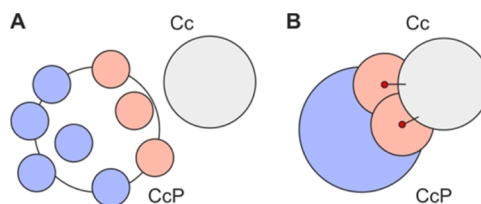


Figure 3. Two labeling schemes for the study of Cc–CcP encounters. (A) CcP is spin-labeled, and the PREs on Cc are detected. The SLs are shown by circles colored pink and blue to indicate the presence and absence of the intermolecular paramagnetic effects, respectively. (B) Cc is labeled with EDTA(Mn²⁺), causing strong PREs (pink) detected on CcP. The CcP region experiencing no effects is colored blue.

and the effects are observed on the smaller one, Cc. In this case, each Cc:CcP–SL experiment probes binding effects in the vicinity of the SL (indicated by colored circles, Figure 3A), while providing no information on the rest of the conformational space. Thus, the exhaustive sampling of the Cc binding over the entire CcP surface requires multiple SLs, which collectively cover the whole interaction space. Moreover, the SLs showing no effects are as important as those giving rise to PREs (blue and red circles in Figure 3A, respectively) as both contribute to the experimental coverage and define the Cc “no-go” zones and its residence areas, respectively. In this setup, an insufficient number of SLs leaves gaps in the encounter maps (white areas in Figure 3A).

The incomplete experimental sampling can be remedied by stronger paramagnetic probes and the inverse labeling scheme, where the probes are attached to the smaller protein, and the intermolecular PREs are detected on the larger binding partner (Figure 3B). In this case, the interaction with Cc is reported by the entire set of CcP backbone amides, affording complete description of the CcP binding surface. This experimental scheme is particularly suitable to the study of Cc–CcP encounters as, according to previous work,¹³ Cc largely maintains frontal orientation while exploring the CcP surface, thus requiring only a few probes to define its rotational degrees of freedom.

To open a door to the CcP-observed NMR experiments, we developed a high-yield *Escherichia coli* expression system for production of isotopically labeled CcP.¹⁶ Protein perdeuteration greatly increased the quality of multidimensional NMR spectra, yielding nearly complete backbone resonance assignments of [²H, ¹³C, ¹⁵N] CcP containing the low-spin ($S = 1/2$), 6-coordinate, CN-ligated heme.¹⁶ Similar spectra of the high-spin ($S = 5/2$), 5-coordinate, resting-state (RS) enzyme—used throughout our earlier studies—suffered from large PREs arising from the native paramagnetic center, leading to significant decrease in signal intensity for the nuclei neighboring the heme group. Therefore, the CcP–RS resonance assignments were obtained via an alternative strategy, relying on pseudocontact shift (PCS)-assisted assignment transfer from the CcP–CN form,¹⁷ and later verified and expanded in a separate work.¹⁸ Finally, a follow-up NMR study¹⁹ validated the Cc–CcP binding in solution and showed that, being in the same redox, spin, and ligation states, the complex of ferrous Cc with CcP(CN) is a good mimic of the catalytically active Cc–CpDI species.

The CcP-observed PRE NMR experiments²⁰ were performed with Cc labeled with EDTA(Mn²⁺) tag, which provides stronger paramagnetic effects and has a higher reduction potential than the nitroxide SL used in our previous work. This setup enables experiments with ferrous Cc (Cc^{red}), not feasible before due to

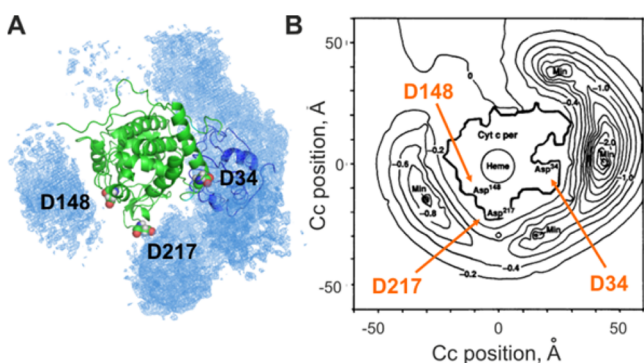


Figure 4. Cc-CcP encounter complex. (A) Atomic probability density map for the overall distribution of Cc molecules obtained in the PRE-based ensemble refinement. The CcP and Cc in the crystallographic orientation are shown in green and blue cartoons, respectively. The CcP residues D34, D148, and D217 are spacefilled and indicated by the labels. (B) Boltzmann-averaged total electrostatic potential energy of the Cc-CcP interaction obtained by Brownian dynamics simulations.²¹ The contours show different energy levels in units of $k_B T$, and the axes indicate the position of the Cc center of mass. Reproduced from ref 20 with permission from the Royal Society of Chemistry and ref 21 with permission from the American Association for the Advancement of Science.

the SL reduction, allowing study of the CcP(CN)-Cc^{red} complex mimicking the active species. Similarly to the Cc-observed experiments, CcP-detected PRE profiles showed strong effects arising from the dominant, crystallographic protein orientation and additional PREs attributed to the encounter state.²⁰ Ensemble refinement of the minor species produced solutions that agreed well with the experimental data and, together with a complementary PCS analysis, provided its population.²⁰ The value of $p = 0.4$ agrees well with that obtained in the earlier MC-based study,¹⁴ validating the use of the simulated Cc-CcP encounters for the p estimates. Interestingly, the encounter complex appeared to be insensitive to changes in redox- and spin-states of the partner proteins, suggesting that its properties are dictated by the protein polypeptides rather than heme cofactors.²⁰

The spatial distribution of the protein–protein orientations sampled in the encounter complex is strikingly similar to that obtained in classic Brownian dynamics (BD) simulations (Figure 4).²¹ This agreement appears even more remarkable as no intermolecular electrostatic forces—which guided the BD simulations—were used in the ensemble refinement protocol, relying solely on the experimental PREs and steric properties of the interacting molecules. However, contrary to the conclusions of the BD work, which imposed the ET reaction criteria to select the successful docking geometries,²¹ the encounter complex described here is essentially ET inactive.²⁰ It appears that while Cc explores the same CcP surface region as that determined in the BD study, the relative orientations of the interacting molecules differ, which explains the disparity in the ET properties of the simulated and experimentally observed protein encounters. Our findings suggest that, rather than directly contributing to the ET activity, the encounter state ensures electrostatically favorable preorientation of the interacting molecules and enables the ensuing reduced dimensionality search of the dominant, functionally active bound form. Compared to the three-dimensional diffusion, such two-dimensional exploration of the binding surface greatly accelerates formation of the productive complex.²

Shifting the Equilibrium between the Major and Minor Species

Further study of the Cc-CcP complex demonstrated that the occupancy of the encounter state can be modulated in a broad range by single point mutations of interfacial residues.²² Using a combination of MC simulations and PRE NMR spectroscopy, it was shown that (1) the Cc T12A mutation decreased the population of the encounter to 10%, compared with 30% in the wild-type (wt) complex; (2) the conservative Cc R13K substitution equalized the two populations; and (3) more dramatically, the Cc R13A mutation reversed the relative occupancies of the stereospecific and the encounter forms, with the latter now being the dominant species with the population of 80%. This finding indicates that the encounter state can make a large contribution to the overall stability of a protein complex. Also, it appears that by adjusting the amount of the encounter through a judicious choice of point mutations, we can remodel the energy landscape of a protein complex and fine-tune its binding specificity.

In a complementary study of the CcP interaction with horse Cc (hCc), a homologue of yeast Cc (yCc) with 63% sequence identity, Ubink and co-workers established that the weaker hCc-CcP complex is much more dynamic than the yCc-CcP system.²³ Interestingly, the conservative hCc K13R mutation—which mimics the native R13 residues of yCc—enhances the binding and yields the dominant form that is remarkably similar to that of the yCc-CcP. (As established by X-ray crystallography,²³ the rmsd for α atoms of the cytochromes in yCc-CcP and K13R hCc-CcP complexes is 0.8 Å.) Subsequent NMR analysis of CcP interactions with wt and K13R hCc revealed less pronounced encounter-derived PREs in the latter, confirming that the dynamic equilibrium in this system is indeed shifted toward the dominant form. Although the authors did not quantify the hCc-CcP encounter populations, qualitative comparison of different PRE profiles broadly supports the above conclusion. Thus, in agreement with the earlier work,²² it appears that the encounter state can be modulated by a single point mutation, and the conservative K13R (hCc) and R13K (yCc) substitutions can interconvert between the “yeastlike” and “horselike” Cc-CcP complexes.

ET Active Protein Encounters

Based on a substantial body of experimental work,⁷ two contrasting models were proposed to explain the Cc-CcP ET activity. According to the first one, the ET occurs only from the Cc bound at the high-affinity CcP site as seen in the X-ray structure of the complex. An alternative mechanism proposes the existence of multiple ET-active protein–protein orientations and postulates that the ET from the Cc bound to a low-affinity site is faster than that in the crystallographic orientation. Ever since, the structure and ET properties of the low-affinity Cc-CcP complex have been a matter of active interest and ongoing debate.⁷

Because of the big (ca. 10 000-fold) difference in the Cc affinities for the two binding sites, biophysical characterization of the ternary complex presented a difficult task,⁷ requiring a highly sensitive technique with a large dynamic range to detect small, low-affinity binding effects in the presence of a dominant, high-affinity signal. To decouple the two binding events, we blocked the high-affinity CcP site by cross-linking it to Cc via a disulfide bond. With the partner proteins locked in the nearly native crystallographic orientation, this covalent cross-link (CL)

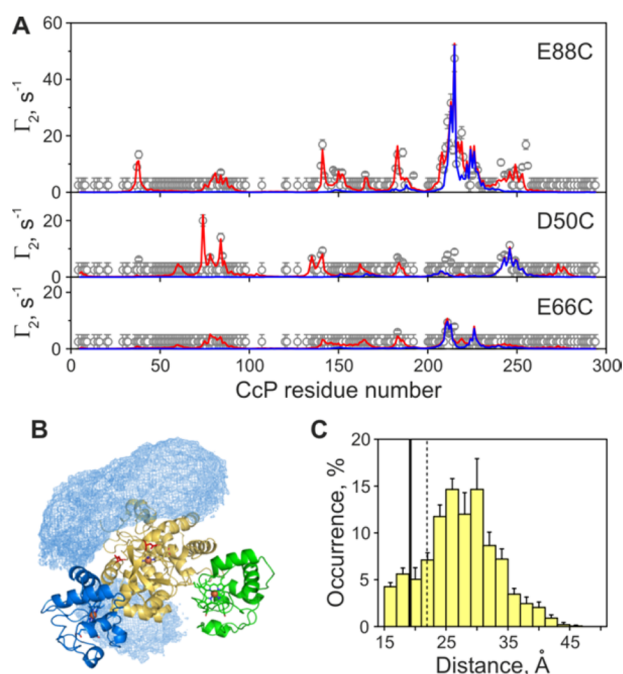


Figure 5. Low-affinity Cc-CcP complex. (A) Intermolecular, CcP-observed PREs for the CL in the complex with Cc paramagnetically labeled at E88C, D50C, and E66C. Plots show measured PREs (open symbols), Γ_2 values back-calculated from the single, lowest-energy CL-Cc structure (blue line), and PREs for the combination of the dominant binding geometry and an ensemble of lowly populated protein-protein orientations (red line). The errors are standard deviations. (B) Cc molecules in the dominant binding geometry (blue cartoon) and multiple minor forms of the low-affinity Cc-CcP complex, displayed as an atomic probability density map for the overall distribution of the Cc heavy atoms. The cross-linked CcP and Cc are colored yellow and green, respectively. (C) Distributions of the Cc-CcP heme-heme distances in the low-affinity complex. The solid and dashed lines indicate the corresponding distances in the crystallographic orientation and the dominant low-affinity binding form, respectively. Reproduced from ref 24. Copyright (2015) by Nature Publishing Group.

allowed PRE NMR study of the low-affinity Cc-CcP interaction in the absence of any binding effects from the high-affinity site.²⁴

Intermolecular PREs from single-cysteine Cc variants labeled with an EDTA(Mn²⁺) tag were observed on the backbone amides of the NMR active, [D,¹⁵N] CcP cross-linked to the NMR silent, natural-abundance Cc (Figure 5A).²⁴ Driven by the combined set of PREs from all three EDTA(Mn²⁺) positions, structure calculations produced a well-defined, low-energy Cc-CL solution (blue cartoon in Figure 5B). However, as can be seen in Figure 5A, not all Γ_2 restraints are accounted for by the single Cc-CL structure, suggesting the presence of lowly populated binding forms giving rise to additional PREs. The ensemble refinement of the minor Cc-CL species consistently produced solutions with bound Cc molecules populating two spatial, electrostatically favorable, regions (Figure 5B). Extending these conclusions to the native, noncovalent Cc-CcP complex, and borrowing the terminology of Hoffman and co-workers,²⁵ we can say that CcP harbors two domains, those binding Cc with high and low affinity and yielding, respectively, the crystallographic Cc-CcP form and the weak complex described here. The low affinity domain contains two binding sites comprising the dominant protein-protein orientation and an ensemble of lowly populated binding geometries, which

summarily account for the observed PREs. Such dynamic view of the ternary CcP-(Cc)₂ complex agrees with conclusions of earlier computational studies and very recent ET kinetics work.^{21,26}

In a broad range of biological systems, the ET rate constants (k_{ET}) are described by an exponential dependence on the distances between the redox centers.²⁷ Thus, to assess the ET properties of the low-affinity Cc-CcP complex, we analyzed the separations between the heme group of Cc and two redox centers in CcP CpdI, the heme oxyferryl and W191⁺ cation-radical. Judging from the large distances of 21 Å (heme-W191) and 22 Å (heme-heme), the dominant low-affinity binding geometry is inactive in the intermolecular ET. In contrast, the conformational ensemble constituting the minor form contains multiple, ET-competent protein-protein orientations with short heme-heme separations of <16 Å (Figure 5C). Calculated as the population-weighted average over all Cc-CcP orientations, $\langle k_{ET} \rangle = 1,950 \pm 450$ s⁻¹ agrees well with the experimentally measured value of 1540 ± 80 s⁻¹ for direct heme-heme ET.^{25,28}

As the high-affinity crystallographic orientation and the encounter state exhibit large separations between the prosthetic groups,^{8,20} it appears that the low-affinity domain alone accounts for the measured heme-heme ET activity.^{25,28}

Taken at the face value, observation of the ET-competent binding geometries seems to contradict the findings of Erman and co-workers, who showed that covalent Cc-CcP complexes with the blocked high-affinity site are inactive toward externally added Cc.²⁹ However, the fact that no enzyme turnover is observed while the heme-to-heme ET is feasible confirms that the catalytic cycle involves ET to W191⁺ and highlights the central role of this CpdI redox intermediate in the CcP function.^{7,9,29} In agreement with this conclusion, the low-affinity complex displays large separations between Cc heme and CcP W191,²⁴ indicating that it does not support the functionally relevant ET activity. While being of great academic interest, the low affinity binding appears to be irrelevant for the physiological function. As it is abolished under the physiological, high ionic strength conditions ($I = 100$ – 150 mM),^{24,30} the cellular enzymatic activity of CcP is expected to rely solely on the intermolecular ET to CpdI W191⁺, taking place from the high-affinity, crystallographic Cc-CcP orientation. However, as the narrow confines of the mitochondrial intermembrane space and macromolecular crowding effects might stabilize the ternary complex, the definitive conclusion on the relevance of the low-affinity site for the physiological ET should await in vivo studies of the Cc-CcP interaction.

■ DYNAMIC DOCKING PARADIGM OF REDOX PROTEIN INTERACTIONS

Supported by theoretical and experimental work on biomolecular encounters across different systems,^{10–12,20,31,32} the prevailing view of protein complex formation is illustrated in Figure 6A. Referred to as “simple docking” (SD), this model posits that preorientation of the interacting partners and conformational sampling of multiple binding geometries in the encounter state lead to the formation of a dominant, functionally active form. Unlike many protein complexes, which require accurate alignment of the binding surfaces in a single, well-defined orientation to carry out their function,³ redox proteins can form multiple productive complexes.³³ In fact, fast ET will occur any time the redox centers of the binding partners are close enough (typically <18 Å)^{27,34} to ensure efficient electron tunneling across the interface. Thus, with

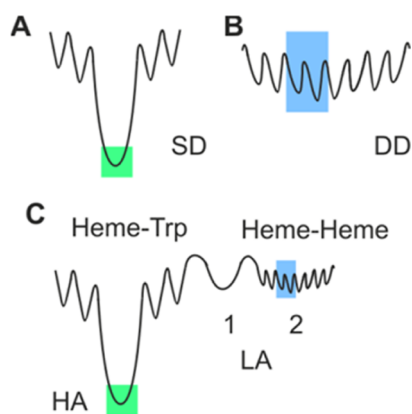


Figure 6. Schematic representation of redox protein binding. Energy landscapes for (A) simple docking (SD), (B) dynamic docking (DD), and (C) Cc-CcP interaction. The ET active conformations are highlighted. In (C), HA and LA denote the high- and low-affinity complexes, respectively, with 1 and 2 indicating the dominant form and the ensemble of minor orientations in the latter. This figure is inspired by papers of Hoffman and co-workers.^{35,41}

the distance between the electron donor and acceptor as the sole most important reaction criterion,²⁷ many protein–protein orientations are expected to be ET active.³³

This view of redox protein interactions engendered the “dynamic docking” (DD) model (Figure 6B), first proposed by Hoffman and co-workers for the complex of myoglobin (Mb) and cytochrome *b*₅ (Cb₅).³⁵ Using a combination of ET kinetics measurements, BD simulations, and NMR spectroscopy, it was shown that—rather than adopting a single, well-defined bound form—this complex consists of multiple, quasi-isoenergetic Mb-Cb₅ orientations, all of which contribute to the overall binding and some of which are ET active.^{35,36} Following this experimental demonstration, a number of other redox protein systems, whose binding and ET properties can be rationalized by the DD model, have been described. These include complexes of cytochrome *f* with its physiological partners plastocyanin³⁷ and cytochrome *c*₆³⁸ and the complex of Cc with adrenodoxin.³⁹ Described as “pure encounters”, the latter two systems were shown to comprise ensembles of lowly populated bound states and bypass formation of a dominant, stereospecific form,^{38,39} suggesting that their ET activity arises solely from a set of transiently bound states. Finally, it was demonstrated that a metabolic network of methylamine oxidation and subsequent electron transport to the terminal oxidase in the soil bacterium *Paracoccus denitrificans* is mediated by redox proteins that form no specific, well-defined complexes.⁴⁰ Consisting of methylamine dehydrogenase, amicyanin, and four *c*-type cytochromes,⁴⁰ most of this interaction network appears to be governed by DD-type complexes exhibiting functional ET activity.

Extending these concepts to the Cc-CcP system, the protein binding can be described by a combination of SD and DD modes (Figure 6C). The high-affinity SD complex consists of the ET-inactive encounter state and the dominant, crystallographic form, enabling functional ET from the Cc heme to the W191* of CcP CpdI.²⁰ At the same time, the low-affinity binding comprises the inactive dominant form and an ensemble of minor DD geometries exhibiting the heme–heme ET.²⁴ While both SD and DD complexes are present at low salt concentrations, the latter is abolished under the physiological, high ionic strength conditions, implying that the functionally relevant ET activity takes place solely in the SD form.

Interestingly, echoing the work on shifting the equilibrium between the dominant and encounter Cc-CcP forms discussed above,^{22,23} Hoffman and co-workers converted a DD complex into the SD one.⁴¹ The authors redesigned the binding interface in the Mb-Cb₅ system to electrostatically stabilize the ET-active protein orientations on its DD energy landscape. This was achieved by three charge-reversal mutations of the Mb surface residues and reconstitution of the protein with a modified heme group, which summarily yielded a +8 change in the Mb charge. BD simulations of the redesigned Mb-Cb₅ complex revealed striking narrowing of the conformational space, consistent with the SD binding mode. Furthermore, the system displayed ultrafast ET kinetics, with intermolecular ET rate constants among the fastest ever measured for a redox protein complex.⁴¹

CONCLUSIONS AND PERSPECTIVES

As demonstrated here, PRE NMR spectroscopy offers detailed description of transient encounters of redox proteins, illuminating their structure and function. Studies of the high-affinity, SD-type, Cc-CcP complex revealed a distinct spatial distribution of protein encounters, suggesting the preferred pathway for the Cc-CcP association (Figure 4). In agreement with the classic BD work,²¹ the proteins explore electrostatically favorable regions of the conformational space on the way to the final bound form. As shown by theoretical and experimental analyses of other biomolecular complexes,^{12,31,32,42,43} the interacting proteins appear to tumble down the electrostatically guided binding funnel, navigating a rugged energy landscape between the fruitful and futile encounters.^{32,43}

From methodological perspective, observation of intermolecular PREs from the smaller, paramagnetically labeled protein on the larger binding partner offers good experimental coverage of the conformational space.^{12,20} Together with stronger paramagnetic probes, such as EDTA(Mn²⁺), this inverse labeling scheme is expected to remedy the insufficient experimental sampling seen in other redox protein complexes.³⁷

Extensively used to analyze ET protein binding,^{21,35,41} BD simulations provide a detailed picture of the macromolecular association and, as confirmed by PRE NMR spectroscopy,²⁰ offer an accurate description of the Cc-CcP encounter state. At the same time, a computationally less demanding MC protocol yields robust estimates of the Cc-CcP encounter populations from the PRE data,^{13,14,22} but breaks down for systems with weaker intermolecular electrostatics. As demonstrated for the ET complex of cytochrome *f* and plastocyanin,³⁷ stabilized by a combination of charge–charge and hydrophobic interactions, electrostatics-based MC simulations show poor agreement with the experimental data. This problem can be alleviated by inclusion of additional energy terms (e.g., van der Waals and desolvation potentials) and a more extensive conformation sampling, which were shown to provide good description of many protein encounters.³¹

With the encounter populations varying from 10–40% in Cc-CcP complexes^{13,14,20,22,23} to nearly 100% in “pure encounter” systems,^{38,39} it appears that low-occupancy states can support functional ET activity and contribute to stability of redox protein complexes. As illustrated here, boundaries between the dominant and the encounter forms become blurred for many dynamic ET systems, which are more aptly described by ensembles of functionally and structurally heterogeneous bound forms of the DD model.

No longer seen as mere exotic curiosities, transient intermediates do govern macromolecular recognition and binding. Apart from purely academic interest, an emerging understanding of their structural and functional properties is expected to inform ongoing bioengineering and drug discovery efforts. Exemplified by the interface redesign work of Hoffman and colleagues,⁴¹ modification of the energy landscape of the encounter state could open a way to more efficient engineering of proteins with desired binding properties or improved design of inhibitors of protein–protein interactions.

AUTHOR INFORMATION

Corresponding Author

*E-mail: ovolkov@vub.ac.be.

Notes

The author declares no competing financial interest.

Biography

Alexander N. Volkov received his M.S. in inorganic chemistry from National Taras Shevchenko University of Kiev in 2000, M.S. in chemistry from Leiden University in 2001, and Ph.D. in life sciences from Leiden University in 2007. After postdoctoral stays at Université Catholique de Louvain, University of Missouri—Columbia, and Vrije Universiteit Brussel, he is a VIB staff scientist running the Jean Jeener NMR Centre in Brussels. His interests include protein–protein interactions, biological electron transfer, and biomolecular NMR.

ACKNOWLEDGMENTS

I acknowledge funding by FWO and thank Marcellus Ubbink and Joris Messens for critical reading of the manuscript.

REFERENCES

- (1) Adam, G.; Delbruck, M. *Structural chemistry and molecular biology*; Rich, A., Davidson, N., Eds.; Freeman: San Francisco, 1968.
- (2) Ubbink, M. The courtship of proteins: understanding the encounter complex. *FEBS Lett.* **2009**, *583*, 1060–1066.
- (3) Lo Conte, L.; Chothia, C.; Janin, J. The atomic structure of protein–protein recognition sites. *J. Mol. Biol.* **1999**, *285*, 2177–2198.
- (4) Crowley, P. B.; Carrondo, M. A. The architecture of the binding site in redox protein complexes: implications for fast dissociation. *Proteins: Struct., Funct., Genet.* **2004**, *55*, 603–612.
- (5) Clore, G. M.; Iwahara, J. Theory, practice, and applications of paramagnetic relaxation enhancement for the characterization of transient low-population states of biological macromolecules and their complexes. *Chem. Rev.* **2009**, *109*, 4108–4139.
- (6) Anthiis, N. J.; Clore, G. M. Visualizing transient dark states by NMR spectroscopy. *Q. Rev. Biophys.* **2015**, *48*, 35–116.
- (7) Volkov, A. N.; Nicholls, P.; Worrall, J. A. R. The complex of cytochrome *c* and cytochrome *c* peroxidase: The end of the road? *Biochim. Biophys. Acta, Bioenerg.* **2011**, *1807*, 1482–1503.
- (8) Pelletier, H.; Kraut, J. Crystal structure of a complex between electron transfer partners, cytochrome *c* peroxidase and cytochrome *c*. *Science* **1992**, *258*, 1748–1755.
- (9) Erman, J. E.; Vitello, L. B. Yeast cytochrome *c* peroxidase: mechanistic studies via protein engineering. *Biochim. Biophys. Acta, Protein Struct. Mol. Enzymol.* **2002**, *1597*, 193–220.
- (10) Volkov, A. N.; Worrall, J. A. R.; Holtzmann, E.; Ubbink, M. Solution structure and dynamics of the complex between cytochrome *c* and cytochrome *c* peroxidase determined by paramagnetic NMR. *Proc. Natl. Acad. Sci. U. S. A.* **2006**, *103*, 18945–18950.
- (11) Iwahara, J.; Clore, G. M. Detecting transient intermediates in macromolecular binding by paramagnetic NMR. *Nature* **2006**, *440*, 1227–1230.
- (12) Tang, C.; Iwahara, J.; Clore, G. M. Visualization of transient encounter complexes in protein–protein association. *Nature* **2006**, *444*, 383–386.
- (13) Volkov, A. N.; Ubbink, M.; van Nuland, N. A. J. Mapping the encounter state of a transient protein complex by PRE NMR spectroscopy. *J. Biomol. NMR* **2010**, *48*, 225–236.
- (14) Bashir, Q.; Volkov, A. N.; Ullmann, G. M.; Ubbink, M. Visualization of the encounter ensemble of the transient electron transfer complex of cytochrome *c* and cytochrome *c* peroxidase. *J. Am. Chem. Soc.* **2010**, *132*, 241–247.
- (15) Iwahara, J.; Schwieters, C. D.; Clore, G. M. Ensemble approach for NMR structure refinement against ¹H paramagnetic relaxation enhancement data arising from a flexible paramagnetic group attached to a macromolecule. *J. Am. Chem. Soc.* **2004**, *126*, 5879–5896.
- (16) Volkov, A. N.; Wohlkonig, A.; Soror, S. H.; van Nuland, N. A. J. Expression, purification, characterization, and solution nuclear magnetic resonance study of highly-deuterated yeast cytochrome *c* peroxidase with enhanced solubility. *Biochemistry* **2013**, *52*, 2165–2175.
- (17) Vanwetswinkel, S.; van Nuland, N. A. J.; Volkov, A. N. Paramagnetic properties of the low- and high-spin states of yeast cytochrome *c* peroxidase. *J. Biomol. NMR* **2013**, *57*, 21–26.
- (18) Schilder, J.; Löhr, F.; Schwalbe, H.; Ubbink, M. The cytochrome *c* peroxidase and cytochrome *c* encounter complex: the other side of the story. *FEBS Lett.* **2014**, *588*, 1873–1878.
- (19) Volkov, A. N.; van Nuland, N. A. J. Solution NMR study of the yeast cytochrome *c* peroxidase: cytochrome *c* interaction. *J. Biomol. NMR* **2013**, *56*, 255–263.
- (20) Van de Water, K.; van Nuland, N. A. J.; Volkov, A. N. Transient protein encounters characterized by paramagnetic NMR. *Chem. Sci.* **2014**, *5*, 4227–4236.
- (21) Northrup, S. H.; Boles, J. O.; Reynolds, J. C. L. Brownian dynamics of cytochrome *c* and cytochrome *c* peroxidase association. *Science* **1988**, *241*, 67–70.
- (22) Volkov, A. N.; Bashir, Q.; Worrall, J. A. R.; Ullmann, G. M.; Ubbink, M. Shifting the equilibrium between the encounter state and the specific form of a protein complex by interfacial point mutations. *J. Am. Chem. Soc.* **2010**, *132*, 11487–11495.
- (23) Bashir, Q.; Meulenbroek, E. M.; Pannu, N. S.; Ubbink, M. Engineering specificity in a dynamic protein complex with a single conserved mutation. *FEBS J.* **2014**, *281*, 4892–4905.
- (24) Van de Water, K.; Sterckx, Y. G. J.; Volkov, A. N. The low-affinity complex of cytochrome *c* and its peroxidase. *Nat. Commun.* **2015**, *6*, 7073.
- (25) Nocek, J. M.; Zhou, J. S.; de Forest, S.; Priyadarshy, S.; Beratan, D. N.; Onuchic, J. N.; Hoffman, B. M. Theory and practice of electron transfer within protein–protein complexes: application to multidomain binding of cytochrome *c* by cytochrome *c* peroxidase. *Chem. Rev.* **1996**, *96*, 2459–2490.
- (26) Page, T. R.; Hoffman, B. M. Control of cyclic photoinitiated electron transfer between cytochrome *c* peroxidase (W191F) and cytochrome *c* by formation of dynamic binary and ternary complexes. *Biochemistry* **2015**, *54*, 1188–1197.
- (27) Moser, C. C.; Keske, J. M.; Warncke, K.; Farid, R. S.; Dutton, P. L. Nature of biological electron transfer. *Nature* **1992**, *355*, 796–802.
- (28) Zhou, J. S.; Hoffman, B. M. Stern–Volmer in reverse: 2:1 stoichiometry of the cytochrome *c* - cytochrome *c* peroxidase electron-transfer complex. *Science* **1994**, *265*, 1693–1696.
- (29) Nakani, S.; Viriyakul, T.; Mitchell, R.; Vitello, L. B.; Erman, J. E. Characterization of a covalently linked yeast cytochrome *c* - cytochrome *c* peroxidase complex: evidence for a single, catalytically active cytochrome *c* binding site on cytochrome *c* peroxidase. *Biochemistry* **2006**, *45*, 9887–9893.
- (30) Cortese, J. D.; Voglino, A. L.; Hackenbrock, C. R. Ionic strength of the intermembrane space of intact mitochondria as estimated with fluorescein-BSA delivered by low pH fusion. *J. Cell Biol.* **1991**, *113*, 1331–1340.
- (31) Kozakov, D.; Li, K.; Hall, D. R.; Beglov, D.; Zheng, J.; Vakili, P.; Schueler-Furman, O.; Paschalidis, I. C.; Clore, G. M.; Vajda, S.

Encounter complexes and dimensionality reduction in protein-protein association. *eLife* **2014**, 3, e01370.

(32) Harel, M.; Spaar, A.; Schreiber, G. Fruitful and futile encounters along the association reaction between proteins. *Biophys. J.* **2009**, 96, 4237–4248.

(33) Volkov, A. N.; van Nuland, N. A. J. Electron transfer interactome of cytochrome *c*. *PLoS Comput. Biol.* **2012**, 8, e1002807.

(34) Page, C. C.; Moser, C. C.; Chen, X.; Dutton, P. L. Natural engineering principles of electron tunnelling in biological oxidation-reduction. *Nature* **1999**, 402, 47–52.

(35) Liang, Z. X.; Nocek, J. M.; Huang, K.; Hayes, R. T.; Kurnikov, I. V.; Beratan, D. N.; Hoffman, B. M. Dynamic docking and electron transfer between Zn-myoglobin and cytochrome *b₅*. *J. Am. Chem. Soc.* **2002**, 124, 6849–6859.

(36) Worrall, J. A. R.; Liu, Y.; Crowley, P. B.; Nocek, J. M.; Hoffman, B. M.; Ubbink, M. Myoglobin and cytochrome *b₅*: a nuclear magnetic resonance study of a highly dynamic protein complex. *Biochemistry* **2002**, 41, 11721–11730.

(37) Scanu, S.; Foerster, J. M.; Ullmann, G. M.; Ubbink, M. Role of hydrophobic interactions in the encounter complex formation of the plastocyanin and cytochrome *f* complex revealed by paramagnetic NMR spectroscopy. *J. Am. Chem. Soc.* **2013**, 135, 7681–7692.

(38) Díaz-Moreno, I.; Hulsker, R.; Skubak, P.; Foerster, J. M.; Cavazzini, D.; Finiguerra, M. G.; Díaz-Quintana, A.; Moreno-Beltrán, B.; Rossi, G. L.; Ullmann, G. M.; Pannu, N. S.; De la Rosa, M. A.; Ubbink, M. The dynamic complex of cytochrome *c₆* and cytochrome *f* studied with paramagnetic NMR spectroscopy. *Biochim. Biophys. Acta, Bioenerg.* **2014**, 1837, 1305–1315.

(39) Xu, X.; Reinle, W.; Hannemann, F.; Konarev, P. V.; Svergun, D. I.; Bernhardt, R.; Ubbink, M. Dynamics in a pure encounter complex of two proteins studied by solution scattering and paramagnetic NMR spectroscopy. *J. Am. Chem. Soc.* **2008**, 130, 6395–6403.

(40) Meschi, F.; Wiertz, F.; Klauss, L.; Blok, A.; Ludwig, B.; Merli, A.; Heering, H. A.; Rossi, G. L.; Ubbink, M. Efficient electron transfer in a protein network lacking specific interactions. *J. Am. Chem. Soc.* **2011**, 133, 16861–16867.

(41) Xiong, P.; Nocek, J. M.; Vura-Weis, J.; Lockard, J. V.; Wasielewski, M. R.; Hoffman, B. M. Faster interprotein electron transfer in a [myoglobin, *b₅*] complex with a redesigned interface. *Science* **2010**, 330, 1075–1078.

(42) Miyashita, O.; Onuchic, J. N.; Okamura, M. Y. Transition state and encounter complex for fast association of cytochrome *c₂* with bacterial reaction center. *Proc. Natl. Acad. Sci. U. S. A.* **2004**, 101, 16174–16179.

(43) Yu, T. K.; Yun, Y. J.; Lee, K. O.; Suh, J. Y. Probing target search pathways during protein-protein association by rational mutations based on paramagnetic relaxation enhancement. *Angew. Chem., Int. Ed.* **2013**, 52, 3384–3388.